Final Draft
of the original manuscript:

Yan, W.; Fang, L.; Weigel, T.; Behl, M.; Kratz, K.; Lendlein, A.:
The influence of thermal treatment on the morphology in differently prepared films of a oligodepsipeptide based multiblock copolymer.
In: Polymers for Advanced Technologies. Vol. 28 (2017) 10, 1339 – 1345
First published online by Wiley: 12.10.2016

https://dx.doi.org/10.1002/pat.3953

The Influence of Thermal Treatment on the Morphology in Differently Prepared Films of a Oligodepsipeptide based Multiblock Copolymer

Wan Yan,[1, 2] *Liang Fang,*[1,#] *Thomas Weigel,*[1] *Marc Behl,*[1, 3] *Karl Kratz,*[1] *Andreas Lendlein*[*1, 2, 3]

[1] Institute of Biomaterial Science and Berlin-Brandenburg Center for Regenerative Therapies, Helmholtz Zentrum Geesthacht, Kantstr. 55, 14513 Teltow, Germany

[2] Institute of Chemistry, University of Potsdam, 14476 Potsdam, Germany

[3] Tianjin University–Helmholtz-Zentrum Geesthacht, Joint Laboratory for Biomaterials and Regenerative Medicine, Kantstr. 55, 14513 Teltow, Germany

[#] Present address: State Key Laboratory of Materials-Oriented Chemical Engineering, College of Material Science and Engineering, Nanjing Tech University, 210009, Nanjing, China.

[*]Email: andreas.lendlein@hzg.de

Abstract

Degradable multiblock copolymers prepared from equal weight amounts of poly(*ε*-caprolactone)-diol (PCL-diol) and poly[oligo(3*S*-*iso*-butylmorpholine-2,5-dione)]-diol (PIBMD-diol), named PCL-PIBMD, provide a phase-segregated morphology. It exhibits a low melting temperature from PCL domains ($T_{m,PCL}$) of 38±2 °C and a high $T_{m,PIBMD}$ of 170±2 °C with a glass transition temperature ($T_{g,PIBMD}$) at 42±2 °C from PIBMD domains.

In this study, we explored the influence of applying different thermal treatments on the resulting morphologies of solution-cast and spin-coated PCL-PIBMD thin films, which showed different initial surface morphologies. Differential scanning calorimetry results and atomic force microscopy images after different thermal treatments indicated that PCL and PIBMD domains showed similar crystallization behaviors in 270±30 μm thick solution-cast films as well as in 30±2 and 8±1 nm thick spin-coated PCL-PIBMD films. Existing PIBMD crystalline domains highly restricted the generation of PCL crystalline domains during cooling when the sample was annealed at 180 °C. By annealing the sample above 120 °C, the PIBMD domains crystallized sufficiently and covered the free surface, which restricted the crystallization of PCL domains during cooling. The PCL domains can crystallize by hindering the crystallization of PIBMD domains via the fast vitrification of PIBMD domains when the sample was cooled/quenched in liquid nitrogen after

annealing at 180 °C. These findings contribute to a better fundamental understanding of the crystallization mechanism of multi-block copolymers containing two crystallizable domains whereby the T_g of the higher melting domain type is in the same temperature range as the T_m of the lower melting domain type.

Keywords: multiblock copolymer; oligodepsipeptides; phase morphology; thermal treatments; crystallization behavior

1. Introduction

Block copolymers including diblock and multiblock copolymers with two immiscible domains is a topic of great interest because of their ability to self-assemble into microphase segregated morphologies, which is widely applied in the field of membranes fabrication,[1] drug delivery,[2] and design of shape-memory polymers[3]. These microphase segregated morphologies can be controlled by varying the composition of the block copolymers.[4] In cases where one or more domains can crystallize, the final morphologies are also related to the thermal transition temperatures i.e. glass transition temperature (T_g) and crystallization temperature (T_c) of constituent domains.[5] When the crystallization occurs in block copolymers composed of one crystallizable domain A and one amorphous domain B, the crystallization of domain A can break out and destroy the previous phase-segregated morphology when $T_{c,A}$ is higher than $T_{g,B}$. Confined crystallization can be observed when $T_{g,B}$ is higher than $T_{c,A}$ since the glassy amorphous phase from domain B obtained the sufficiently strong tendency of phase-segregation.[5, 6] The segregated block copolymers composed of two semi-crystalline domains exhibit more complex crystallization behaviors because of the additional competition between the crystallization of the two crystallizable domains.[7-9] Crystallizations of two domains can occur simultaneously when the two domains obtained well-separated T_cs or separately if their T_cs are close.[10, 11] By application of different thermal treatments, the final morphology of semi-crystalline block copolymers can be altered[12-15], and in this way changes their mechanical properties[16, 17], degradation rate[18] or shape-memory properties[19]. For example, a two stage crystallization took place when the segregated diblock copolymer polyethylene-poly(*L*-lactide) was slowly cooled from the melt state to temperatures below than the T_cs of both crystallizable domains, but when a rapid cooling process was applied coincident crystallization occurred.[20]

Most research activities on block copolymers having two crystallizable domains concentrate on copolymers with well-separated T_cs which are not overlapping with any T_g of the materials. However, more morphological richness could be provided by block copolymers containing two crystalline domains and, more specifically, a T_g of one domain close to the T_c of the other domain. The restriction from glassy amorphous domain and the competition of two crystalline domains need to be considered. Therefore, a multiblock copolymer synthesized from equal weight amounts of oligomeric starting materials oligo(*ε*-caprolactone)-diol (PCL-diol) and oligo(3*S*-*iso*-butylmorpholine-2,5-dione)-diol (PIBMD-diol), coupled by trimethyl hexamethylene diisocyanate (TMDI), named PCL-PIBMD, was studied in the current work, which has been introduced to reveal an excellent dual-shape-memory property and has potential applications as degradable biomaterials.[21-23] In the PCL-PIBMD block polymers, both crystalline PCL domains with a melting temperature ($T_{m,PCL}$) of 38±2 °C and amorphous PIBMD domains with a glass transition temperature ($T_{g,PIBMD}$) at 42±2 °C can act as switching domains, while physical netpoints determining the permanent shape are formed by PIBMD crystallites with a high $T_{m,PIBMD}$ of 170±2 °C. For the purpose of exploring the influence of applying different thermal treatments on the resulting morphologies of multiblock copolymers containing two crystallizable domains whereby the T_g of the higher melting component is in the same temperature range as the T_m of the lower melting component, the thermal properties of solution-cast films after three kinds of thermal treatments were measured by differential scanning calorimetry (DSC). The morphologies of a solution-cast film and two spin-coated thin films with varying film thicknesses before and after three thermal treatments were visualized by atomic force microscopy (AFM). The surface element compositions of spin-coated films were analyzed using X-ray photoelectron spectroscopy (XPS).

2. 2. Experimental

2.1 Materials

PCL-PIBMD was synthesized from equal weight amounts of poly(*ε*-caprolactone) diol (M_n = 2700 g·mol^{-1}) and poly[oligo(3*S*-*iso*-butylmorpholine-2,5-dione)] diol (M_n = 9300 g·mol^{-1}) reacted with trimethyl hexamethylene diisocyanate using dibutyltin dilaurate as catalyst according to the method described previously.[21] The M_n of PCL-PIBMD was 53000 g·mol^{-1} with a polydispersity of 2.0 as determined by multi-detector gel permeation chromatography via universal calibration.

2.2 Film preparation

Solution-casting. 2.28 g PCL-PIBMD was dissolved in 50 ml chloroform overnight at ambient temperature with a polymer concentration of 3 *wt*%. The solution-casting was carried out in glass petri dishes (diameter = 80 mm, Duran Group, Wertheim, Germany) with the subsequent evaporation of the solvent for 5 days. The resulting film thickness was 270±30 μm, measured using a thickness gauge (Hans Schmidt, Waldkraiburg, Germany).

Spin-coating. PCL-PIBMD was dissolved in 10 ml chloroform with a concentration of 0.1 and 0.05 *wt.*%. Thin films on silicon wafers, which were cleaned using the standard RCA method, were prepared using a spin coater (WS-650SZ-6NPP/A1/AR1, Laurell Technologies Co., USA) under spin speeds of 4000 and 1000 rpm, respectively. The films thicknesses were determined by purposely applying a scratch to the polymer film and subsequent AFM topography imaging in the vicinity area of the scratch, which were 30 and 8 nm, respectively.

Thermal treatments. Three thermal treatments were applied to the prepared solution-cast film and spin-coated films in sequence: (1) Annealing at 180 °C: the samples were cooled slowly in air after being heated to 180 °C using a hot plate and kept for 5 min; (2) Annealing at 120 °C: the samples were cooled slowly in air after being heated to 120 °C using a hot plate and kept for 5 min. (3) Quenched in liquid nitrogen (LN): the samples were quickly moved into LN after being heated to 180 °C using a hot plate and kept for 5 min, and then the samples were took out of LN and kept in air.

2.3 Characterization Methods

Differential scanning calorimetry (DSC) experiments were conducted on a Netzsch DSC 204 Phoenix (Selb, Germany) at heating and cooling rates of 10 $K \cdot min^{-1}$ in sealed aluminum pans. The thermal properties of the prepared solution-casted film and the solution-casted films after three thermal treatments were detected by first cooling from RT to 0°C then heating from 0 °C to 200 ºC. The crystallization temperatures (T_c), melting temperatures (T_m) and the related melting enthalpies (ΔH) were determined from the heating runs.

Atomic force microscopy (AFM) (Multimode with NanoScope V Controller, Veeco Instruments Inc., USA) with a temperature controller (Veeco Thermal application controller, Veeco Instruments Inc., USA) was performed to obtain the morphologies of solution-cast and spin-coated films. Silicon cantilevers (OLYMPUS OMCL AC200TS-R3), with a tip radius of 7 nm and back and side angles of 35º and 18º, a spring constant of 9 $N \cdot m^{-1}$ and a driving frequency of 150 kHz were used for measurements with a typical scan rate of 0.8–1.0 Hz. The morphologies of samples at 20 °C were measured at three different positions, while one specific region of interest was selected to detect the morphological variation during heating gradually from 20 to 60 °C. The estimated error for temperature was ±2 °C.

X-ray photoelectron spectroscopy (XPS) was conducted with Axis Ultra DLD from Kratos Analytical Ltd., Manchester, UK. Survey scans were recorded with monochromatic Al k-α radiation at 15kV and 5mA, field of view 700 × 300 μm, with pass energies of 160 eV and under use of charge compensator. All samples were measured at a detector angle of 0°. The spectra were analyzed using the software CasaXPSTM (Version 2.3.16, Casa Software Ltd., UK). The content of *N* and *C* elements on the free surface of spin-coated films were measured in order to calculate the PCL and PIBMD contents on the surface on the basis of the different ratios of *N*/*C* elements in PCL and PIBMD segments as shown in the following:

$$N/C \text{ ratio in PIBMD segments} = x(PIBMD) \times f(IBMD) + x(TMDI) \times f(TMDI) \quad (1)$$

$$N/C \text{ ratio in PCL segments} = x(PCL) \times f(CL) + x(TMDI) \times f(TMDI) \quad (2)$$

Here, *f* is the *N*/*C* ratio in each monomer, while *x* is the fraction of relevant component in PCL or PIBMD segments.

3. Results and Discussion

PCL-PIBMD thin films with thicknesses of 270±30 μm, 30±2 nm and 8±1 nm were prepared via solution-casting or spin-coating technique. Their surface morphologies and thermal properties after different thermal treatments were discussed to clarify the crystallization behaviors of both domains and the influence from thermal treatments.

3.1 Initial morphologies of solution-cast and spin-coated PCL-PIBMD films

The surface morphologies of PCL-PIBMD solution-cast film and spin-coated films immediately

after preparing, were characterized by AFM at 20 and 60 °C, which is below and above $T_{m,PCL}$ and $T_{g,PIBMD}$, respectively. Figure 1a shows the morphology from solution-cast film, where polymer crystals as typical spherulites composed of highly ordered edge-on lamellae can be observed. By heating to 60 °C (Figure 1 d), the large spherulites originated from PIBMD domains did not change evidently, while small PCL crystals, which were confined within the crystalline lamellae of PIBMD domains, were melted. Different from the solution-cast film, thin films with nano-scale thickness showed distinct morphologies due to the effect of surface energy and interfacial tensions of both segments with the substrate. As illustrated in Figure 1b, the PCL-PIBMD spin-coated film with a thickness of 30 nm presented a weak microphase separated morphology with few crystals after casting, which proved the PCL and PIBMD domains are only partially miscible and the crystallization of both domains were hindered because of the influence from the surface tension. When the sample was heated to 60 °C where the mobility of polymer chains increased by beyond the $T_{g,PIBMD}$ around 42±2 °C (determined by DMTA, not shown here), small rod-like crystals of PIBMD domains generated on the film surface (Figure 1e). Thus, the PIBMD crystals can break-out and enrich at the air/polymer interface. Similarly, the PCL-PIBMD spin-coated film with a thickness of 8 nm showed no crystals on the film surface and presented a surface morphology with holes on the surface due to its extremely low thickness (Figure 1c). As shown in Figure 1f, edge-on rod-like crystals appeared on the surface after heating to 60 °C, which belongs to crystalline PIBMD domains.

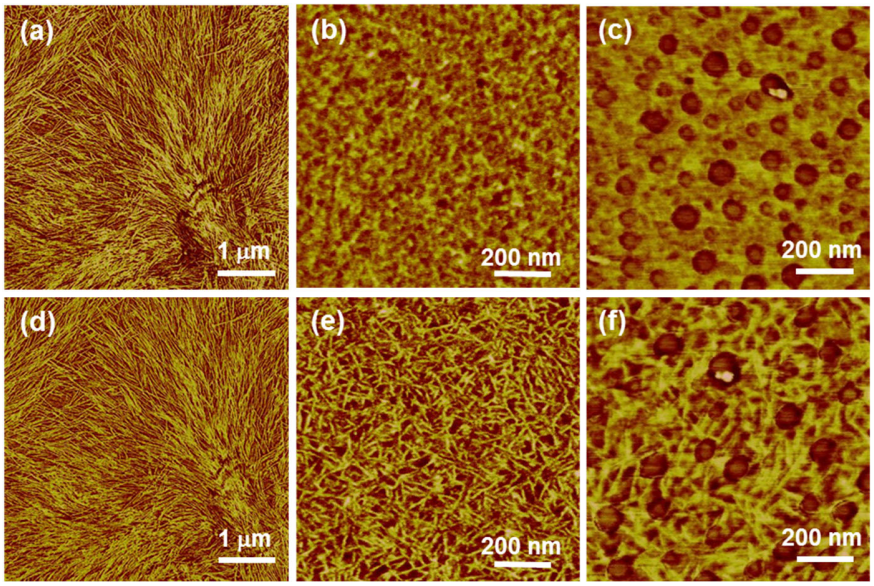

Figure 1. AFM phase images of PCL-PIBMD (a, d) solution-cast film with a thickness of 270 µm and spin-

coated films with a thickness of (b, e) 30 nm and (c, f) 8 nm. The images were scanned at (a-c) 20 °C and (d-f) 60 °C.

3.2 Thermal treatments on solution-cast and spin-coated PCL-PIBMD films

Three thermal treatments were first applied to the solution-casted films as described in the experimental part. The thermal properties achieved for the solution-cast films after application of the thermal treatments determined by DSC are presented in Figure 2 and the results are summarized in Table 1. Two clear melting peaks at 35±1 and 169±1 °C corresponding to T_m of PCL and PIBMD domains can be observed for the film prepared by solution-casting. After annealing the sample at 180 °C, which is above $T_{m,PIBMD}$, a new coldcrystallization peak ($T_{cc,PIBMD}$) belonging to PIBMD domains was found during cooling at 114±1 °C, while the typical melting peaks of PCL and PIBMD crystals were still observed at 39±1 and 168±1 °C. The appearance of a cold crystallization peak in PIBMD domains ($T_{cc,PIBMD}$) during heating at temperatures above $T_{g,PIBMD}$ is relevant to their insufficient crystallization during the preliminary cooling procedure. Thus, the PIBMD chains reorganized into their ordered crystal structures after reheating the sample above $T_{g,PIBMD}$. More importantly, as demonstrated in Table 1, the melting enthalpy of PCL crystalline phase in the film after 180 °C annealing was only 1±1 $J \cdot g^{-1}$ compared to the case of film after casting having 12±2 $J \cdot g^{-1}$ melting enthalpy of PCL crystals. This result indicated that the crystallization of PCL domains was significantly restricted by PIBMD domains during the cooling procedure. To clarify the effect of PIBMD crystals on the crystallization of PCL domains, the second thermal treatment method was to anneal the PCL-PIBMD sample at 120 °C, which is above $T_{cc,PIBMD}$. The reorganization of PIBMD chains occurred and a sufficient crystallization of PIBMD domains was achieved, presenting no cold crystallization peak of PIBMD domains in the DSC curve. In addition, no PCL melting peaks can be observed from the DSC curve, suggesting that the crystallization of PCL domains was totally restricted during the cooling steps because of the appearance of more PIBMD crystals formed during the annealing. Finally, after the sample was heated to 180 °C and quenched in LN, an evident and broad melting peak at the range of 20 to 70 °C with a maximum at 42±1 °C was obtained during the heating scan, showing an increasing melting enthalpy of PCL crystals of 38±1 $J \cdot g^{-1}$. A significant shift of the cold crystallization peak of PIBMD domains towards the lower temperature (90±1 °C) was also observed. The reason could be that the nucleation and growth of PIBMD crystals were hindered by quick vitrification of PIBMD segments during the rapid quenching using LN. Therefore, their restriction effect on the

crystallization of PCL domains was negligible. Furthermore, the $T_{cc,PIBMD}$ shifted from 114±1 to 90±1 °C, demonstrating that the PIBMD chains started to rearrange into ordered crystalline structures earlier resulting from its fast vitrification. It has to be mentioned that no crystallization peak can be observed from the cooling curve for all measurements due to the weak and slow crystallization of PIBMD domains and the restriction from PIBMD crystals to PCL crystallization.

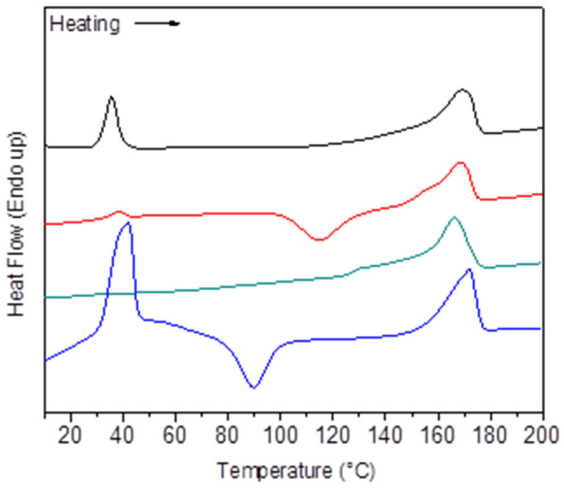

Figure 2. DSC heating curves of PCL-PIBMD solution casted films with different thermal histories: (black) thermal equilibrium; (red) annealing at 180 °C for 2 min and cooling to RT; (green) annealing at 120 °C for 2 min and then cooling to RT; and (blue) annealing at 180 °C for 2 min and quenching in LN. All curves represent the first scan.

Table 1. Thermal properties of PCL-PIBMD after different thermal treatments.

Thermal Treatment	$T_{m,PCL}$*	$\Delta H_{m,PCL}$*	$T_{cc,PIBMD}$*	$\Delta H_{cc,PIBMD}$*	$T_{m,PIBMD}$*	$\Delta H_{m,PIBMD}$*
	°C	J·g^{-1}	°C	J·g^{-1}	°C	J·g^{-1}
after casting	35±1	12±2	-	-	169±1	22±2
Annealing at 180 °C	39±1	1±1	114 ±1	-12±2	167±1	13±2
Annealing at 120 °C	-	-	-	-	167±1	26±2
Quenching in LN	42±1	38±2	90±1	-19±2	172±1	22±2

*: Melting temperatures (T_m), cold crystallization temperatures (T_{cc}) and enthalpy (ΔH) were calculated from the DSC curves. The estimated error for T is ±1 °C and for ΔH is ±2 J·g^{-1}.

The surface morphologies of solution-cast and spin-coated PCL-PIBMD films with different thicknesses after three thermal treatments were visualized by AFM as illustrated in Figure 3. In the case of the solution-cast film, some rod-like crystals belonging to PIBMD domains generated on the film surface after annealing at 180 °C (Figure 3(I)a) since these crystals grew gradually after heating the sample to 60 °C (Figure 3(I)d). Slight changes can be observed in Figure 3(I)b and e when the sample was annealed at 120 °C, which indicated that PIBMD domains were sufficiently crystallized and the crystallization of PCL domains were restricted by the PIBMD crystals totally. Finally, when the sample was annealed at 180 °C and fast cooled in LN, small PCL crystals appeared on the film surface as indicated in Figure 3(I)c, which melted during heating to 60 °C (Figure 3(I)f). PIBMD crystals then generated and richened on the top surface. These observations from AFM images matched the DSC results.

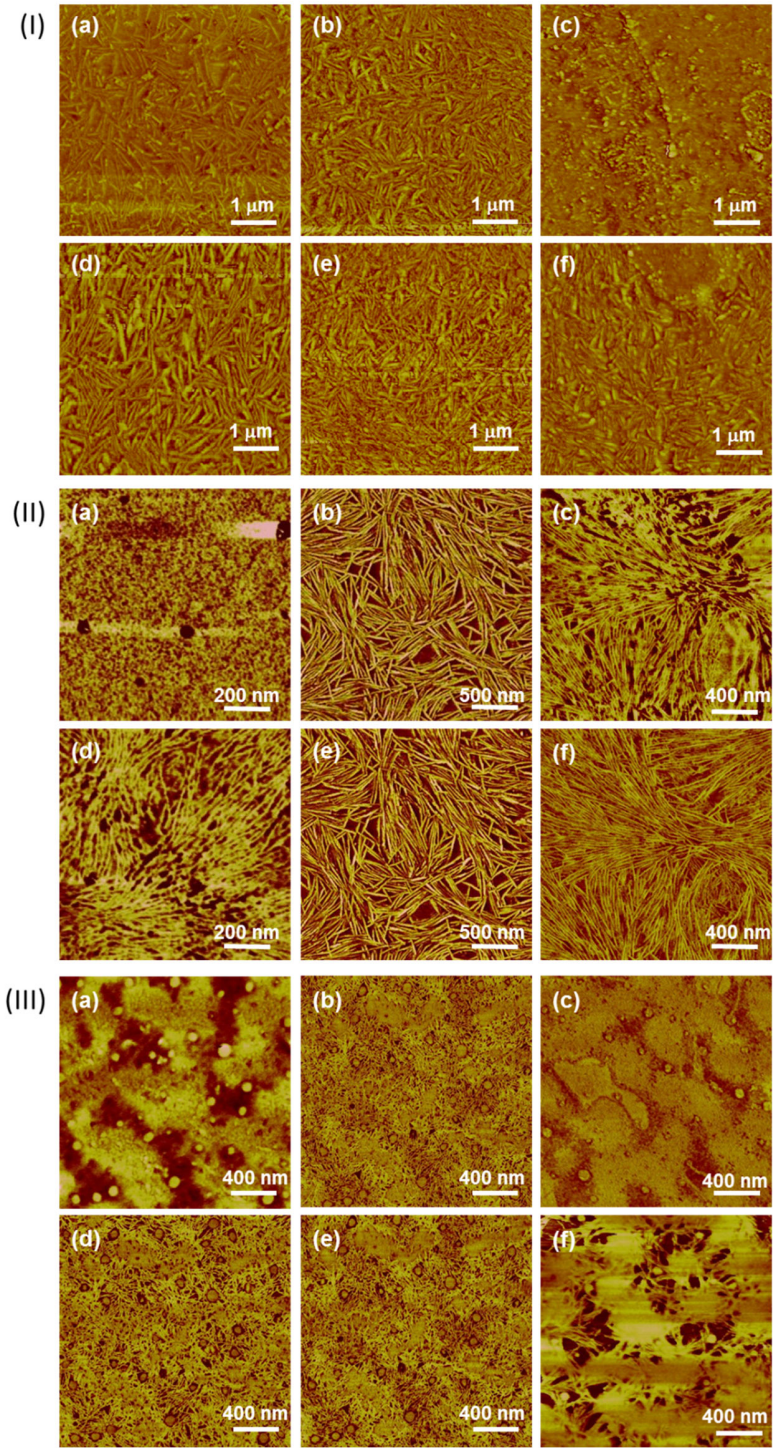

Figure 3. AFM phase images of PCL-PIBMD (I) solution cast film with a thickness of 270 µm and spin-coated films with a thickness of (II) 30 nm and (II) 8 nm 300 µm after three thermal treatments: (a, d) annealing at 180 °C; (b, e) annealing at 120 °C and (c, f) quenching in LN. The images were scanned at (a-c) 20 °C and (d-f) 60 °C.

For the spin-coated thin film with a thickness of 30 nm, many small crystal nuclei were found after annealing at 180 °C as observed in Figure 3(II)a. Fibrillar PIBMD lamellae are observed to branch out significantly from small crystal nuclei when the temperature was raised to 60 °C (Figure 3(II)d). No PCL can be observed after annealing since the restriction from PIBMD domains. Figure 3(II)b and e showed the PCL-PIBMD spin-coated thin films annealed at 120 °C and cooled down to RT. Numerous fibrillar PIBMD crystals were observed, occupying the free surface, and no changes can be observed after heating to 60 °C. It was further proved that the PCL crystallization was totally hindered by the PIBMD crystals. To facilitate the crystallization of PCL domains, the thin film was heated to 180 °C and quenched in LN. Large amounts of flat-on PCL crystals were found among the edge-on lamellae as shown in Figure 3(II)c. Then the PCL crystals melted, while the PIBMD lamellae started to grow and broke out to form large spherulites when the temperature was heated to 60 °C, as presented in Figures 3(II)f.

Similar phenomena could be observed for the spin-coated film with a thickness of 8 nm. After annealing to 180 ºC, spinodal-like pattern with few PIBMD fibril crystals were observed (Figure 3(III)a). Fibrous PIBMD lamellae were found nucleating from the edge of the protruded spinodal-like patterns and growing towards the top of spinodal-like patterns, when the temperature was increased to 60 ºC (Figure 3(III)d). PCL crystals, however, could not be observed because of the hindrance from PIBMD crystals. The crystallization of PIBMD domains was achieved after annealing at 120 ºC due to the cold crystallization and PCL crystallization was totally restricted. Therefore, no changes can be seen between Figure 3(III)b and e, which were scanned at 20 and 60 °C, respectively. As indicated in Figure 3(III)c, when the sample was heated to 180 °C and then quenched in LN, both of flatten-on PCL crystals and few PIBMD lamellae were found on the top surface. Followed by the melting of PCL crystals at 60 °C, the growth of PIBMD crystals extended to the top of the spinodal-like patterns (Figure 3(III)f).

In summary, the spin-coated thin films exhibited a similar crystallization behavior as the solution-cast film after applying different specific thermal treatments. The existing PIBMD crystals can restrict the crystallization of PCL domains, while different thermal treatments can result in a distinct degree of crystallinity of PCL and PIBMD domains in PCL-PIBMD films.

3.3 Morphologies of spin-coated PCL-PIBMD thin films

Previous investigations have shown that diblock copolymer thin films should form a highly oriented lamellar structure parallel to the substrate with a period of L_0 equal to the thickness of two phase-separated lamellae. For a stable film with uniform thickness, the quantization constraint in uniform thickness of (n + 1/2) L_0 or nL_0, where n is an integer, should be initially fulfilled. Relief structures with islands of height L_0 or hole of depth L_0 are generated on the surface after equilibrium when the film thickness does not fulfill this constraint.[24, 25] Therefore, the surface topographies of spin-coated PCL-PIBMD thin films with the thickness of 30 and 8 nm after annealing at 180 °C for 30 min were examined using AFM at room temperature. The temperature, 180 °C, is above the melting temperature of both PCL and PIBMD domains, which enabled the thermal equilibrium without the influence of structural force. As shown in Figure 4a and b, the leftmost point of samples was scratched prior to annealing in order to expose the layer of substrate, where is used as a reference to measure the height of each layer. A bicontinuous spinodal pattern was observed in the film with an initially thickness of 30 nm (Figure 4a). The cross-sectional profiles of this AFM height image indicated that the spinodal pattern with a height of 24.1 ± 2.8 nm occurred on a layer of height around 13.2 ± 2.3 nm. When the thickness of polymer film reduced to around 8 nm, spinodal pattern of height ~ 21.2 ± 2.5 nm (Figure 4b) were found in the AFM height images. Therefore, it can be assumed that the multiblock copolymer PCL-PIBMD thin films followed the rules to form oriented lamellar structures parallel to the substrate, where the two domains were phase separated into a lamellar structure with a L_0 around 23±1 nm or an asymmetric wetting occurred to form islands or holes of height equaled to 1/2L_0 ~ 12±1 nm.

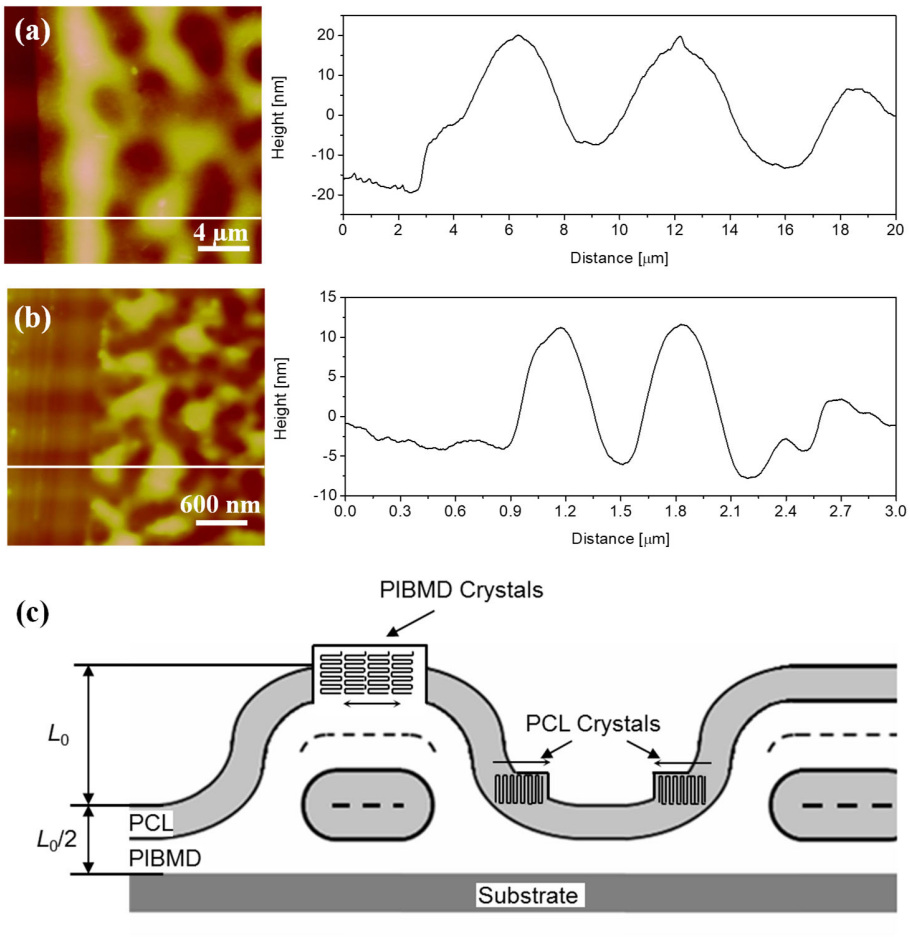

Figure 4. AFM height images and cross-sectional profiles of annealed PCL-PIBMD spin coated films with a thickness of (a) 30 nm and (b) 8 nm. The films on the left side are removed gently using a blade. (c) Schematic structures for semi-crystalline PCL-PIBMD thin films on silicon wafers.

The surface element compositions of these two spin-coated films were determined by XPS measurements on which the composition ratio of PCL domains was calculated as described in the experimental part. The result demonstrated that the fraction of PCL on the free surfaces of spin-coated film with a thickness of 30 was 84±1%. A pronounced silicon signal coming from silicon wafer substrate was detected for the film of 8 nm thickness since the depth of XPS detection is around 10 nm. In this particular case XPS cannot provide information about the composition of the thin polymer film. Another spin-coated PCL-PIBMD film with thickness of 18±2 nm (not shown here) was measured and 78±2% of PCL domains wetted on the film surface. Therefore, it can be inferred that the PCL domains prefer to enrich at the free surface after casting, while PIBMD

crystals can break out from the previously ordered lamellar structures and then spread on the free surface after annealing above the $T_{cc,PIBMD}$. The reason for the PCL domains enriched on the free surface could be the low molecular weight of PCL blocks compared to PIBMD blocks.[26] With the combination of AFM and XPS results, spin-coating films can form a structure in an ordered state as schematically depicted in Figure 4c. A parallel ordered lamellar structure with a period of L_0 ~23±1 nm was generated in the spin-coated films, with PCL and PIBMD segments wetting the free surface and the underlying substrate, respectively. Relief structure of holes or islands with a height around L_0 may appear on the surface to achieve the minimum surface and interface energy. The crystallization of PIBMD domains can break out from the previously ordered structures and then enriched at the air/polymer interface.

4. Conclusions

In the present work, morphologies of PCL-PIBMD films with different thicknesses produced by solution-casting and spin-coating method were investigated. Large PIBMD spherulites with confined PCL crystals were found spreading on the surface in solution-cast films, while PCL domains were found to enrich in the top layer of the surface after spin-coating, where PIBMD crystals can break out and cover on the free surface under heating to 60 °C. Three thermal treatments were applied to the PCL-PIBMD films to clarify the crystallization behavior of PCL and PIBMD domains. All soultion-cast and spin-coated films showed similar crystallziation behaviours and different thermal treatments can result in a distinct degree of crystallinity of PCL and PIBMD domains in PCL-PIBMD. The results indicated that the existing PIBMD crystals can restrict the crystallization of PCL domains. The PIBDM crystallization, however, can also be hindered by the fast vitrification of the PIBMD amorphous phase when quenched in LN, generating more PCL crystals. In nanoscale thin films, the PCL segments enriched at the free surface, while PIBMD segments wetted the underlying substrate to form parallel ordered lamellar structure with a period of L_0 ~ 23±1 nm. By annealing the sample above the cold crystallization temperature of PIBMD domains, the PIBMD crystals broke the ordered layer structure and covered the free surface. This work illustrated the crystallization behavior of the kind of block copolymer containing two crystalline domains whereby the T_g of the higher melting domain is in the same temperature range as the T_m of the lower melting domain. In addition the different thermal treatments provided a way to control the degree of crystallinity of PCL and PIBMD domains as

well as surface morphologies by adjusting their crystallization processes. These findings contribute to a fundamental understanding of the crystallization mechanism of copolymers comprising two crystallizable domains and the influence of a glass transition in the same temperature region on their crystallization behavior.

Acknowledgements

The authors thank Mr. Olaf Lettau for synthesis of PCL-PIBMD and Ms. Susanne Schwanz for technical support. This work was supported by the Helmholtz-Association through programme-oriented funding as well as through a fellowship for W.Y. by the Helmholtz Graduate School for Macromolecular Bioscience (VH-GS-503).

References

[1] R. M. Dorin, W. A. Phillip, H. Sai, J. Werner, M. Elimelech, U. Wiesner, *Polymer* **2014**, 55, 347.
[2] M. T. Peracchia, R. Gref, Y. Minamitake, A. Domb, N. Lotan, R. Langer, *Journal of Controlled Release* **1997**, 46, 223.
[3] M. Behl, J. Zotzmann, A. Lendlein, *Advances in Polymer Science* **2010**, 226.
[4] C. Vasilev, G. Reiter, S. Pispas, N. Hadjichristidis, *Polymer* **2006**, 47, 330.
[5] L. Mandelkern, *Crystallization of Polymers: Volume 2, Kinetics and Mechanisms*, Cambridge University Press, Cambridge, 2004.
[6] W.-N. He, J.-T. Xu, *Progress in Polymer Science* **2012**, 37, 1350.
[7] A. J. Müller, J. Albuerne, L. Marquez, J.-M. Raquez, P. Degée, P. Dubois, J. Hobbs, I. W. Hamley, *Faraday discussions* **2005**, 128, 231.
[8] R. Castillo, A. Müller, *Progress in Polymer Science* **2009**, 34, 516.
[9] J. E. Báez, A. Ramírez-Hernández, Á. Marcos-Fernández, *Polymers for Advanced Technologies* **2010**, 21, 55.
[10] M.-C. Lin, H.-L. Chen, W.-B. Su, C.-J. Su, U.-S. Jeng, F.-Y. Tzeng, J.-Y. Wu, J.-C. Tsai, T. Hashimoto, *Macromolecules* **2012**, 45, 5114.
[11] R. V. Castillo, A. J. Muller, J.-M. Raquez, P. Dubois, *Macromolecules* **2010**, 43, 4149.
[12] Y. Yanagihara, N. Osaka, S. Murayama, H. Saito, *Polymer* **2013**, 54, 2183.
[13] Q. Tian, I. Krakovský, G. Yan, L. Bai, J. Liu, G. Sun, L. Rosta, B. Chen, L. Almásy, *Polymers* **2016**, 8, 197.
[14] S. L. Li, F. Wu, Y. Yang, Y. Z. Wang, J. B. Zeng, *Polymers for Advanced Technologies* **2015**, 26, 1003.
[15] I. Hamley, P. Parras, V. Castelletto, R. V. Castillo, A. J. Müller, E. Pollet, P. Dubois, C. Martin, *Macromolecular Chemistry and Physics* **2006**, 207, 941.
[16] Y. Yanagihara, N. Osaka, S. Iimori, S. Murayama, H. Saito, *Materials Today Communications* **2015**, 2, e9.
[17] J. Ruokolainen, G. H. Fredrickson, E. J. Kramer, C. Y. Ryu, S. F. Hahn, S. N. Magonov, *Macromolecules* **2002**, 35, 9391.
[18] Z. Gan, K. Kuwabara, H. Abe, T. Iwata, Y. Doi, *Polymer degradation and stability* **2005**, 87, 191.
[19] K. Kratz, U. Voigt, A. Lendlein, *Advanced Functional Materials* **2012**, 22, 3057.

[20] R. V. Castillo, A. J. Müller, M.-C. Lin, H.-L. Chen, U.-S. Jeng, M. A. Hillmyer, *Macromolecules* **2008**, 41, 6154.
[21] Y. Feng, M. Behl, S. Kelch, A. Lendlein, *Macromolecular Bioscience* **2009**, 9, 45.
[22] W. Yan, L. Fang, U. Noechel, K. Kratz, A. Lendlein, *Express Polymer Letters* **2015**, 9, 624.
[23] W. Yan, L. Fang, U. Noechel, K. Kratz, A. Lendlein, *Journal of Polymer Science Part B: Polymer Physics* **2016**, 54, 1935.
[24] Y. Li, Y.-L. Loo, R. A. Register, P. F. Green, *Macromolecules* **2005**, 38, 7745.
[25] G.-D. Liang, J.-T. Xu, Z.-Q. Fan, S.-M. Mai, A. J. Ryan, *The Journal of Physical Chemistry B* **2006**, 110, 24384.
[26] J. Rodríguez-Hernández, C. Drummond, *Polymer Surfaces in Motion: Unconventional Patterning Methods*, Springer, International Publishing Switzerland, 2015.